Analyzing Wave Energy Dissipation Efficiency of Oyster Farm Structures: Implications for Coastal Protection and Electricity Generation

Manassanan Namman[1,*] Nattakamol Jaichumchuen[1] Jirasuta Thutakit[1] Duangrudee Kositgittiwong[1] Chaiwat Ekkawatpanit[1] Wongnarin Kompor[1] and Chanchai Petpongpan[1]

[1]Department of Civil Engineering, Faculty of Engineering, King Mongkut's University of Technology Thonburi, Bangkok, Thailand.
**Corresponding author; E-mail address: manassanan.namman@gmail.com*

Abstract

Thailand's coastal areas along both the Gulf of Thailand and the Andaman Sea are significantly impacted by coastal erosion, which affects economic activities such as tourism and coastal fisheries. Although Thailand has developed renewable energy sources such as hydropower, wind, and solar, wave energy remains largely underutilized due to relatively high costs and uncertainty about its potential across different regions. Given the dual challenges of coastal erosion and the underuse of wave energy, there is increasing interest in integrated solutions that address both issues simultaneously. This study focuses on reducing wave energy and mitigating coastal erosion by using oyster farm poles as wave energy dissipating structures. Four pole arrangements were tested: a rectangle, two trapezoidal patterns (with either the longer or shorter parallel side facing the waves), and a diamond shape. These were categorized into two groups based on void ratio. The results indicate that the rectangular and diamond shapes are most effective under deep wave conditions, while both trapezoidal arrangements perform best under transitional waves. In terms of the relationship between wave energy loss and electricity generation, at a still water level of 0.45 meters, electricity output ranged from 4.7 to 6.6 W/m with an average wave energy loss of approximately 2%. At 0.40 meters, electricity output ranged from 4.6 to 7.2 W/m with an average energy loss of approximately 2.5%.

Keywords: Coastal erosion, Wave energy, Oyster farm poles

1. Introduction

1.1 Rationale of the Study

Thailand has a coastline of approximately 3,151 kilometers across 23 provinces, divided into two regions: the Gulf of Thailand (2,039.78 kilometers) and the Andaman Sea (1,111.35 kilometers). The coastline greatly benefits the economy and environment, supporting tourism, fisheries, aquaculture, and industry. However, despite the implementation of protective measures in some locations, coastal erosion has become a serious issue. Erosion is driven by climate change, sea level rise, and human activities that disrupt coastal ecosystems. According to previous research [2], around 823 kilometers of shoreline have been affected, with 69.74 kilometers unprotected, 753.32 kilometers protected by structures, and 2,328.07 kilometers stable. In some areas, protection efforts have reduced erosion, such as in Phetchaburi province. Coastal erosion affects communities by causing land loss and damaging natural barriers like mangroves. While hard protection structures can help, they may also lead to further erosion or ecological damage. Meanwhile, rising energy costs have increased interest in clean, renewable sources such as wave energy, particularly along the Andaman coast, where wave conditions are suitable.

This study aims to develop an oyster reef farm model that can both dissipate wave energy and support wave energy conversion. The investigation evaluates different pile arrangements, measures wave transmission coefficients, and tests the potential for electricity generation using the Sea Oyster converter in a laboratory wave flume. The goal is to identify effective designs that enhance coastal protection and promote sustainable energy, with applications in Thailand and beyond.

1.2 Objectives

1. To investigate the optimal arrangement of oyster farming poles for enhancing wave energy dissipation efficiency.
2. To assess the wave energy dissipation and wave transmission characteristics of different oyster pole configurations.
3. To evaluate and compare the electricity generation potential and energy conversion efficiency of various oyster pole arrangements.

1.3 Scopes of Study

1. The behavior of waves through the application of dimensional analysis and similarity are done by simulating wave flow behavior using a physical model.
2. This study employs a 1:10 scale based on Froude similarity, using the dimensions of the flume to represent the shoreline distance and designing wave conditions based on dimensionless π-terms. The generated waves were selected to match target wave steepness ($\frac{H_1}{\lambda_1}$) and relative depth ($\frac{d}{\lambda_1}$), ensuring that the experimental conditions represent deep and transitional wave environments studied in this research.
3. The wave energy dissipation efficiency and transmission coefficients are analyzed through various model arrangements and their impact on coastal erosion.

2. Theory

2.1 Coastal Erosion

Coastal erosion is the result of sediment being displaced from the shoreline by natural forces such as waves, currents, tides, wind, and extreme weather events. These processes are often intensified by human activities that disrupt the natural sediment balance.

Natural causes include wave action that removes sediment, seasonal monsoon winds that alter sediment transport patterns, ocean currents that reshape nearshore zones, and tidal fluctuations that move sediment along the coast. Human-induced causes involve coastal development projects like ports, factories, and hotels that disturb natural coastal dynamics, as well as inappropriate land use, such as converting mangrove forests into shrimp farms, which weakens shoreline stability and accelerates erosion.

2.2 Coastal Erosion Prevention and Mitigation Measures

Coastal erosion significantly impacts marine and coastal ecosystems, disrupts local livelihoods, and causes economic losses. As a result, various coastal protection and mitigation measures have been implemented from the past to the present. Different management approaches have been adopted depending on site-specific conditions, leading to the development of 3 main categories of measures, which are further divided into 8 specific types, as shown in Fig. 1.

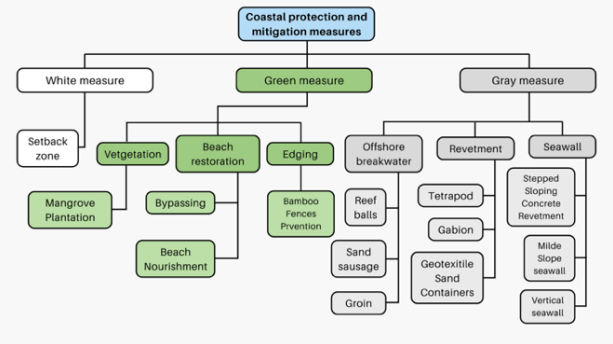

Fig. 1 Coastal protection and mitigation measures [1]

1) White Measure

White measures involve setting buffer zones and restricting land use to reduce erosion and remove contributing structures. Though effective in high-risk areas, implementation is difficult due to high costs and land use conflicts.

2) Green Measure

Green measures focus on preserving and stabilizing the coastline naturally without significant impacts on adjacent areas. This approach is suitable for sheltered coasts with low waves and gently sloping shores. Examples include Vegetation, Beach Restoration, and Edging.

- Bamboo Wave Barriers serve as a coastal protection measure designed to reduce wave intensity before waves reach the shoreline. These barriers enhance sediment deposition behind the structure, accelerating the formation of stable coastal areas. Bamboo barriers are particularly suitable for regions with relatively low wave heights, making them an effective and eco-friendly solution for mitigating coastal erosion.

3) Gray Measure

Gray measures are engineering solutions aimed at stabilizing coasts in open-sea environments with high waves and steep slopes. Examples include Offshore Breakwaters, Revetment and Seawalls.

2.3 Theory of Wave

Ocean waves are formed by wind blowing across the sea surface, with their size depending on wind speed and the distance it travels without interruption. They are defined by their period, wavelength, height, and direction. Waves from nearby winds are called sea waves, while those from distant storms are swell waves. Most wind-driven waves are gravity waves with periods under 25 seconds. In deep water, wave speed is related to wave period, and water particles move in circular paths. As waves approach shallow water, they slow down due to seabed friction, causing wave heights to increase through shoaling until they eventually break.

2.3.1 Wave Components

A wave consists of several key components.

1. The crest is the highest point of a wave, while the trough is the lowest.

2. The wave height (H) is the vertical distance between the crest and the trough.

3. the wavelength (λ) is the horizontal distance between two consecutive crests.

4. The wave period (T) refers to the time it takes for one wave crest to travel to the position of the next crest.

5. The wave frequency (f) is the number of waves that occur per second, calculated as shown in Eq. (1).

$$f = \frac{1}{T} \tag{1}$$

6. The wave speed (c) is the rate at which a wave propagates forward and can be determined using the Eq. (2).

$$c = \frac{\lambda}{T} \tag{2}$$

7. The amplitude (a) of a wave is measured from the mean sea level to the wave crest, and the wave height (H) is defined as twice the amplitude, calculated as shown in Eq. (3).

$$H = 2a \tag{3}$$

8. The wave frequency (ω) is given by Eq. (4).

$$\omega = \frac{2\pi}{T} \tag{4}$$

9. Water particles move in circular orbits along the wave surface with a velocity defined in Eq. (5).

$$v = \frac{2\pi a}{T} = \frac{\pi H}{T} = \frac{\lambda}{T} = \lambda f \tag{5}$$

10. Wave steepness is the ratio between wave height (H) and wavelength (L), defined in Eq. (6).

$$steepness = \frac{H}{L} \tag{6}$$

2.3.2 Wave Size

Waves vary in shape and size based on ocean conditions, location, and season. Their size is mainly influenced by wind speed (W), fetch (F), and duration (D). Wind speed is the wind's velocity, fetch is the distance it travels without interruption, and duration is how long it blows in a constant direction. Wave size is typically measured by wave period (T) and wave height (H), as shown in Equation (7) [3].

$$T, H = f(W, F, D) \tag{7}$$

2.3.3 Wave Transmission Coefficient (K_t)

The wave transmission coefficient (K_t) is determined by calculating the average transmitted wave height on the shoreward side of the breakwater for each measurement point. This value is then compared to the incident wave height (H_i), which is obtained from wave probes positioned offshore of the breakwater in previous sections [4] and can be represented symbolically as Eq. (8)

$$K_t = \frac{H_t}{H_i} \tag{8}$$

Where K_t = Wave Transmission Coefficient
H_i = Wave height at the front of the model structure (m)
H_t = Wave height at the back of the model structure (m)

3. Methodology

This study evaluates the efficiency of oyster reef structures through simulations using experimental testing in a wave flume. The wave flume has a width of 0.6 meters, a depth of 0.8 meters, and a length of 12.0 meters. The oyster reef pile structures are designed and analyzed in four main configurations, with the

installation of a Wave Energy Converter (WEC) to assess the overall system performance. The detailed study procedures are shown in Fig. 2.

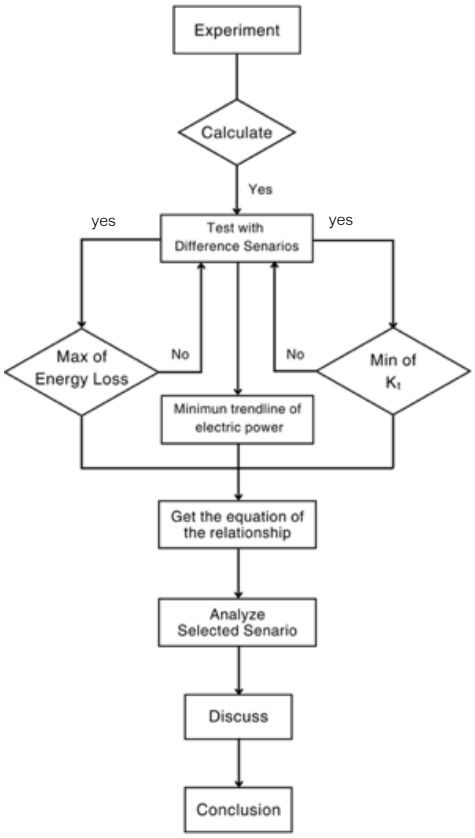

Fig. 2 Research Methodology for Evaluating Oyster Reef Pile Structures and Wave Energy Converter Performance

3.1 Testing Tools and Equipment

3.1.1 Wave Flume

The wave flume, located in the Water Resources Engineering Laboratory at King Mongkut's University of Technology Thonburi. It has a width of 0.60 meters, a height of 0.80 meters, and a length of 12 meters. wavelength both before and after passing through the structure.

3.1.2 Wave Generator

The HF 560-080 Wave Generator is installed at the start of the flume and produces waves using a bottom-hinged flap plate. The upper part of the flap connects to a crankshaft rod driven by a gear system and a 3-horsepower motor. The crankshaft has adjustable slots allowing a maximum stroke of 0.3 meters. Wave frequency, up to 50 Hz, is controlled through the generator.

3.2 Types of Oyster Reefs and Design of Oyster Reef Pile Structure Arrangements

The efficiency of various oyster reef structures using key parameters was compared, including dimensionless height ($\frac{h_s}{d}$) and dimensionless width ($\frac{B}{H_i}$), to evaluate the wave transmission coefficient (K_t). The experimental results shown that the oyster shell bag had the lowest wave transmission coefficient among all tested structures. This is due to its compact shape and low porosity, which enhance wave energy dissipation more effectively than other structures. Based on these findings, the study selected the most effective oyster reef structures for wave energy reduction that are also feasible for implementation in this experiment. The selected structure is pile structures. [6]

An efficiency test on wave energy reduction using oyster reef pile structures was conducted, where four different arrangements were tested based on the number of pile rows 1, 2, 3, and 4 rows. The results showed that a three-row oyster reef pile structures with short wave periods and a narrow pile angle relative to the breakwater achieved the highest wave energy reduction, approximately 53%. [5]

For this study, four oyster reef pile structure arrangements were designed using a 1:10 scale model to determine suitable dimensions and water depths for testing in the wave flume. The structural layouts, as illustrated in the following Figs. 3 - 6.

1) Module 1 follows a rectangular arrangement, consisting of 3 rows with 9 piles each, totaling 27 piles. The details are illustrated in Fig. 3.

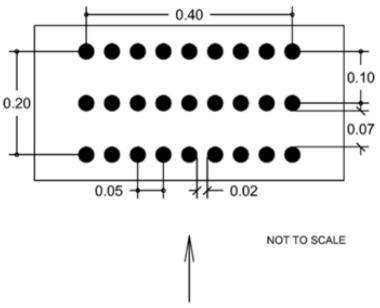

Fig. 3 Plan of Oyster Reef Pile Structure in Rectangle Pattern – Module 1

2) Module 2 follows a trapezoidal arrangement, with the shorter parallel side facing the wave direction. It consists of 3 rows, with 7 piles in the first row, 9 piles in the second row, and 11 piles in the third row, totaling 27 piles. The details are illustrated in Fig. 4.

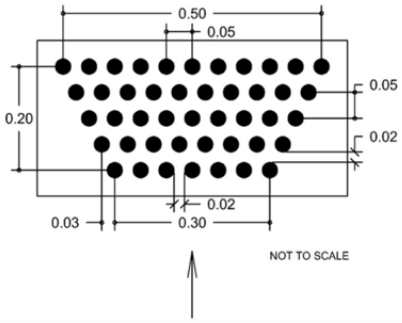

Fig. 4 Plan of Oyster Reef Pile Structure in Trapezoidal Pattern – Module 2

3) Module 3 follows a trapezoidal arrangement, but with the longer parallel side facing the wave direction. It consists of 3 rows, with 11 piles in the first row, 9 piles in the second row, and 7 piles in the third row, totaling 27 piles. The details are illustrated in Fig. 5.

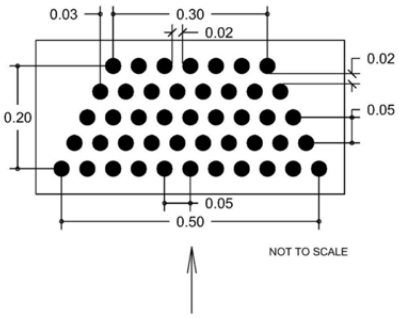

Fig. 5 Plan of Oyster Reef Pile Structure Trapezoidal Pattern – Module 3

4) Module 4 follows a rectangular arrangement with a staggered layout, consisting of 6 rows with 9 piles each, totaling 27 piles. The details are illustrated in Fig. 6.

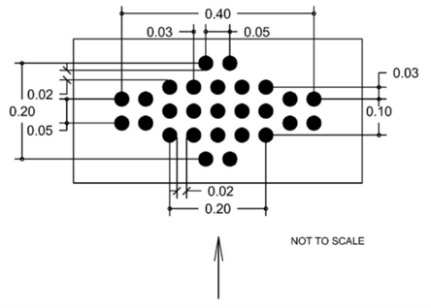

Fig. 6 Plan of Oyster Reef Pile Structure in Diamond Shape – Module 4

3.3 Data Collection

Wave data were collected by two methods: direct measurement and image processing. As both approaches produced nearly identical results, image processing was adopted for consistency. During the experiments, videos were recorded and processed using a Python script that applied Canny edge detection to enhance the water surface boundary. Every 30 seconds, a frame was selected, and the crest and trough positions were manually marked based on the enhanced image. Wave heights were then determined using grid size 2 cm x 2 cm on the flume wall for calibration.

3.4 Experimental Procedure

This study involved testing four different oyster reef structural arrangements under still water depths of 0.35, 0.40, and 0.45 meters. For each depth, waves were generated at frequencies of 25, 30, and 35 Hz, resulting in a total of 36 test cases. The experimental steps included 1) Installing the oyster reef structure in the wave flume. 2) Calibrating the wave generator height. Generating waves and observing wave–structure interactions 3) Recording the experiment using a video camera. 4) Analyzing wave heights through image processing to calculate wave transmission coefficients.

3.5 Result Analysis

This experiment is based on the assumption that the wave motion in still water is steady, with no changes during movement at a specific location. Therefore, measurements are taken at two points.

1) In front of the model structure

2) Behind the model structure

The collected data are used to analyze the relationship between variables to determine the efficiency of wave energy

dissipation and how these variables relate to each other. These relationships are compared to the performance of the wave energy dissipation by the model structure under regular wave conditions

4. Result

4.1 Energy Dissipation from Various Oyster Pile Models under Different Depths

This study tested wave behavior in a flume with a width of 0.60 meters, height of 0.80 meters, and length of 12 meters. The test was conducted at three still water depths: 0.35, 0.40, and 0.45 meters, along with wave generator frequencies of 25, 30, and 35 Hz.

Wave velocity was analyzed by examining its linear relationship with the motor frequency of the HF 560–080 Wave Generator at still water depths of 0.35, 0.40, and 0.45 meters, as represented by Equation 12.

For still water depth (d) = 0.35 meters

$$y = -0.0317x + 2.2432 \quad (12a)$$

For still water depth (d) = 0.40 meters

$$y = -0.0279x + 2.0829 \quad (12b)$$

For still water depth (d) = 0.45 meters

$$y = -0.0235x + 1.8932 \quad (12c)$$

4.2 The influence of relative depth on the wave transmission coefficient

The experimental results show that relative depth ($\frac{d}{\lambda_1}$) has a significant influence on the wave transmission coefficient (K_t). As relative depth increases, K_t tends to decrease, indicating improved wave energy dissipation. Module 3 and Module 1 are more effective in deep wave conditions, while Module 2 and Module 4 perform better under transitional wave conditions with sharper peaks and greater variability, as shown in Fig. 8.

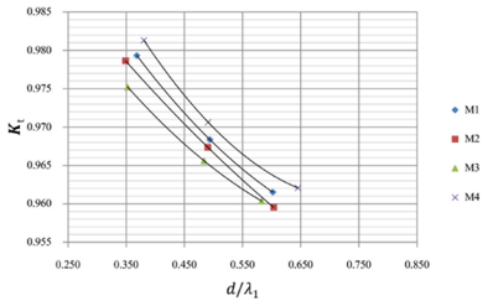

(a) At still water depth (d) = 0.45 meters

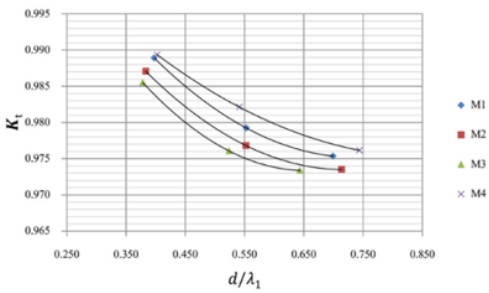

(b) At still water depth (d) = 0.40 meters

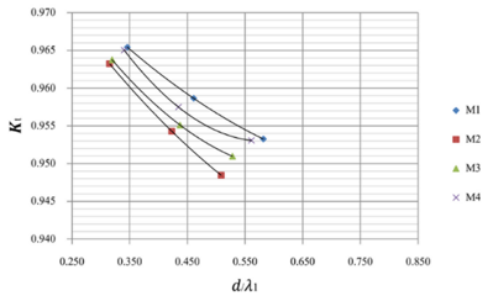

(c) At still water depth (d) = 0.35 meters

Fig. 8 The influence of relative depth on the wave transmission coefficient

4.3 The influence of relative depth on the specific energy dissipation efficiency (Energy Loss)

Experimental results reveal that relative depth ($\frac{d}{\lambda_1}$) has a direct and positive influence on wave energy dissipation efficiency. As relative depth increases, energy dissipation also improves. Module 3 and Module 1 perform well under deep wave conditions with stable wave characteristics, while Module 2 and Module 4 are more effective under transitional wave conditions with higher variability, as illustrated in Fig. 9.

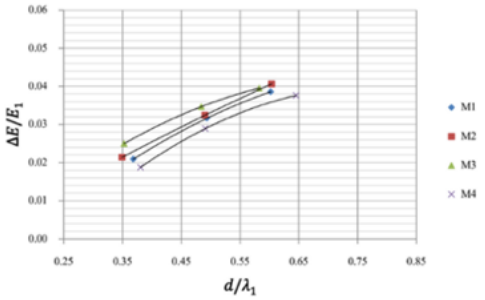

(a) At still water depth (d) = 0.45 meters

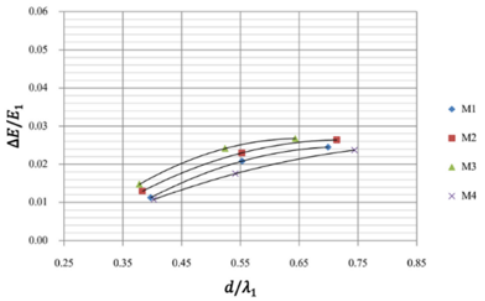

(b) At still water depth (d) = 0.40 meters

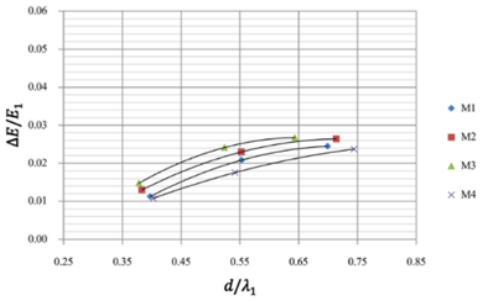

(c) At still water depth (d) = 0.35 meters

Fig. 9 The influence of relative depth on the specific energy dissipation efficiency (Energy Loss).

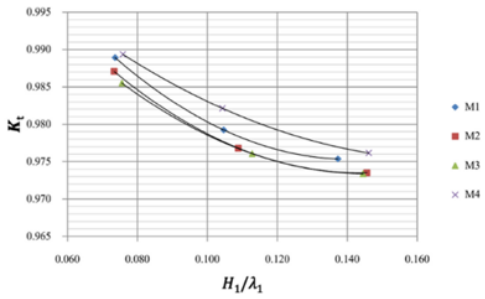

(a) At still water depth (d) = 0.45 meters

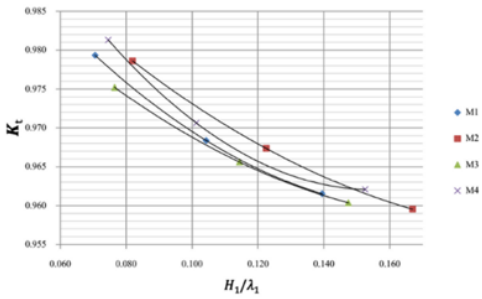

(b) At still water depth (d) = 0.40 meters

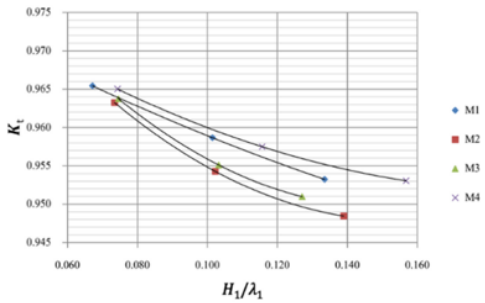

(c) At still water depth (d) = 0.35 meters

Fig. 10 influence of wave steepness on the wave transmission coefficient

4.4 The influence of wave steepness on the wave transmission coefficient

This experiment examined the effect of wave steepness ($\frac{H_I}{\lambda_I}$) on the wave transmission coefficient (K_t). Results show that as steepness increases, K_t decreases, indicating better wave attenuation. Module 3 and Module 1 perform well under deep, stable wave conditions, while Module 2 and Module 4 are more effective under high-steepness, transitional waves with sharper forms as shown in Fig. 10.

4.5 The influence of wave steepness on the specific energy dissipation efficiency

The results show that energy dissipation efficiency increases with wave steepness ($\frac{H_I}{\lambda_I}$). From the graphs Module 3 and Module 1 are more effective for deep waves with low steepness. Module 2 and Module 4 perform better under high steepness or transitional waves as shown in Fig. 11.

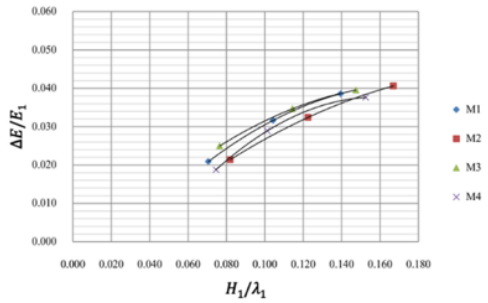

(a) At still water depth (d) = 0.45 meters

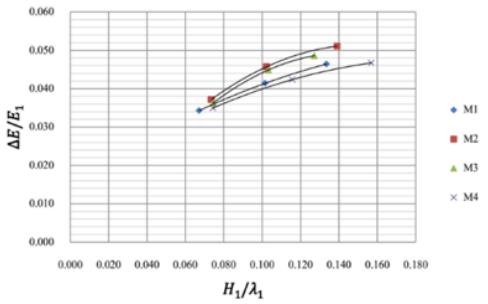

(b) At still water depth (d) = 0.40 meters

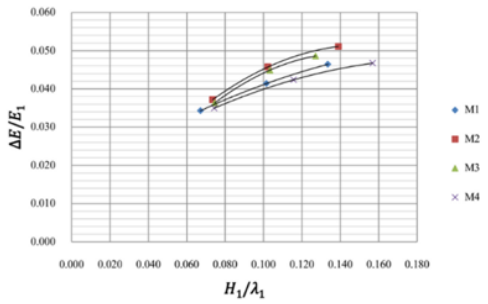

(c) At still water depth (d) = 0.35 meters

Fig. 11 the influence of wave steepness on the specific energy dissipation efficiency.

4.6 The relationship between the wave transmission coefficient and specific energy dissipation efficiency

The analysis establishes a relationship between the wave transmission coefficient and the specific energy dissipation efficiency, as represented by the two equations shown on Eq. 13 and 14.

$$\frac{\Delta E}{E_I} = -0.992(K_t)+0.992 \quad (13)$$

$$\frac{\Delta E}{E_I} = -K_t+1 \quad (14)$$

4.10 The relationship between electrical power production and wave energy loss at still water level 0.45 m

The relationship between electrical power production and wave energy loss at a still water level of 0.45 meters was analyzed by plotting energy loss against electrical output, resulting in a minimum trendline and a fitted equation, as shown in Eq. 15.

$$y = 0.7067x^{0.6216} \quad (15)$$

The findings reveal varying performance across module configurations. Modules 1 and 4 maintain low energy loss under moderate power conditions. Module 2 shows reduced efficiency as power increases, while Module 3 performs better under higher wave energy input, as illustrated in Fig. 12.

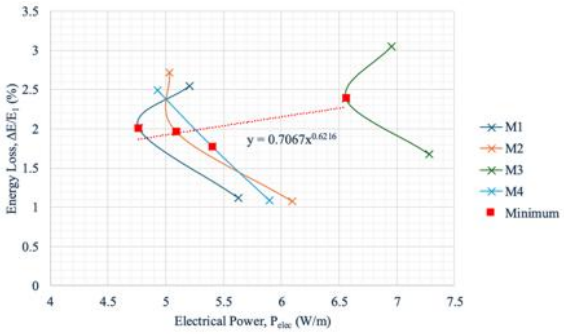

Fig. 12 The relationship between electrical power production and wave energy loss at still water level 0.45 m.

4.11 The relationship between electrical power production and wave energy loss at still water level 0.40 m.

The relationship between electrical power production and wave energy loss at a still water level of 0.40 meters was analyzed by plotting energy loss values against electrical power output. The resulting data produced a minimum trendline and a fitted equation, which is expressed in Eq.16 and shown graphically in Fig. 13.

$$y = 0.6539x^{0.7993} \quad (16)$$

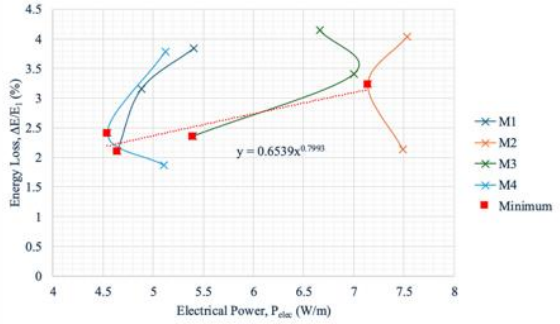

Fig. 13 The relationship between electrical power production and wave energy loss at still water level 0.40 m.

5. Conclusions

This study evaluated the wave energy dissipation performance of different oyster farming pole arrangements using a 1:10 scale model under both deep and transitional wave conditions. Among the configurations, Module 1, which shares the same pole density as Module 4, showed the best performance under deep wave conditions, while Module 2, similar in density to Module 3, was most effective under transitional conditions. These results highlight the importance of adapting pole arrangements to match specific wave environments to maximize energy dissipation.

The study also examined the relationship between electrical power output and wave energy loss at still water levels of 0.45 m and 0.40 m. At 0.45 m, energy loss increased gradually with power output, making it more suitable for low- to medium-power applications. At 0.40 m, a steeper increase in energy loss was observed, suggesting better efficiency at higher power outputs.

Overall, these findings offer practical guidance for designing oyster reef farms that serve dual purposes: protecting coastlines and generating renewable energy. For Thailand, where coastal erosion is a growing concern, such integrated systems could support sustainable coastal management efforts by reducing wave impacts while contributing to local energy needs.

Nonetheless, there are limitations to this work. The experiments were conducted in a laboratory setting at a reduced scale, which cannot fully replicate the complexity of natural coastal environments, such as variable wave climates, sediment dynamics, and biological interactions. Future studies should include field-scale trials and long-term monitoring to better evaluate the real-world performance and durability of these systems.

Acknowledgement

This research was supported by the Civil Engineering Diamond Scholarship provided by the Department of Civil Engineering, King Mongkut's University of Technology Thonburi (KMUTT), for the academic year 2024. The researcher gratefully acknowledges this support, which made the completion of this study possible.

References

[1] กัดเซาะชายฝั่ง - สถานภาพการกัดเซาะชายฝั่ง ปี พ.ศ. 2564 - ระบบฐานข้อมูลทรัพยากรทางทะเลและชายฝั่ง กรมทรัพยากรทางทะเลและชายฝั่ง. (n.d.). Demo. https://km.dmcr.go.th/c_55/d_19692

[2] กัดเซาะชายฝั่ง - สถานภาพการกัดเซาะชายฝั่ง ปี พ.ศ. 2565 - ระบบฐานข้อมูลทรัพยากรทางทะเลและชายฝั่ง กรมทรัพยากรทางทะเลและชายฝั่ง. (n.d.). Demo.

[3] *โครงการปักไม้ไผ่ชะลอคลื่นป้องกันการกัดเซาะชายฝั่ง 7 - MarineThai*. (n.d.). บริษัท เอ. แอนด์ มารีน (ไทย) จำกัด. https://www.marinethai.net/โครงการปักไม้ไผ่/โครงการปักไม้ไผ่ชะลอค-16/

[4] Ahmadian, A. S. (2016). *Numerical models for submerged breakwaters: Coastal Hydrodynamics and Morphodynamics.* Butterworth-Heinemann., pp. 127–143.

[5] Intasupa, A., Ouypornprasert, W., Ratanamanee, P., Jarupongsakul, T., & Sojisuporn, P. (2010). An efficiency test on wave energy reduction of piled breakwaters using physical model. *Journal of Environmental Research*, 32(2), 50-51

[6] Xu, W., Tao, A., Wang, R., Qin, S., Fan, J., Xing, J., Wang, F., Wang, G., & Zheng, J. (2024). Review of wave attenuation by artificial oyster reefs based on experimental analysis. *Ocean Engineering,* 298, 117309.